

RESEARCH ARTICLE

Approaching an experimental electron density model of the biologically active *trans*-epoxysuccinyl amide group—Substituent effects vs. crystal packing

Ming W. Shi¹ | Scott G. Stewart¹ | Alexandre N. Sobolev¹ | Birger Dittrich² |
Tanja Schirmeister³ | Peter Luger⁴ | Malte Hesse⁵ | Yu-Sheng Chen⁶ | Peter R. Spackman¹ |
Mark A. Spackman¹ | Simon Grabowsky^{1,5} 

¹School of Chemistry and Biochemistry, The University of Western Australia, Perth, WA, Australia

²Anorganische Chemie und Strukturchemie, Heinrich-Heine-Universität Düsseldorf, Düsseldorf, Germany

³Institut für Pharmazie und Biochemie, Johannes-Gutenberg-Universität Mainz, Mainz, Germany

⁴Institut für Chemie und Biochemie, Anorganische Chemie, Freie Universität Berlin, Berlin, Germany

⁵Fachbereich 2—Biologie/Chemie, Institut für Anorganische Chemie und Kristallographie, Universität Bremen, Bremen, Germany

⁶ChemMatCARS, The University of Chicago, Argonne, IL, USA

Correspondence

Simon Grabowsky, Fachbereich 2—Biologie/Chemie, Institut für Anorganische Chemie und Kristallographie, Universität Bremen, Leobener Str. NW2, 28359 Bremen, Germany
Email: simon.grabowsky@uni-bremen.de

Funding information

Divisions of Chemistry (CHE) and Materials Research (DMR), National Science Foundation, Grant/Award Number: NSF/CHE-1346572. Danish National Research Foundation, Grant/Award Number: DNRF-93. German Research Foundation (Deutsche Forschungsgemeinschaft DFG), Grant/Award Number: DI 921/6-1. GR 4451/1-1. Australian Research Council (ARC), Grant/Award Number: DE140101330. DP130103488.

Abstract

The *trans*-epoxysuccinyl amide group as a biologically active moiety in cysteine protease inhibitors such as loxistatin acid E64c has been used as a benchmark system for theoretical studies of environmental effects on the electron density of small active ingredients in relation to their biological activity. Here, the synthesis and the electronic properties of the smallest possible active site model compound are reported to close the gap between the unknown experimental electron density of *trans*-epoxysuccinyl amides and the well-known function of related drugs. Intramolecular substituent effects are separated from intermolecular crystal packing effects on the electron density, which allows us to predict the conditions under which an experimental electron density investigation on *trans*-epoxysuccinyl amides will be possible. In this context, the special importance of the carboxylic acid function in the model compound for both crystal packing and biological activity is revealed through the novel tool of model energy analysis.

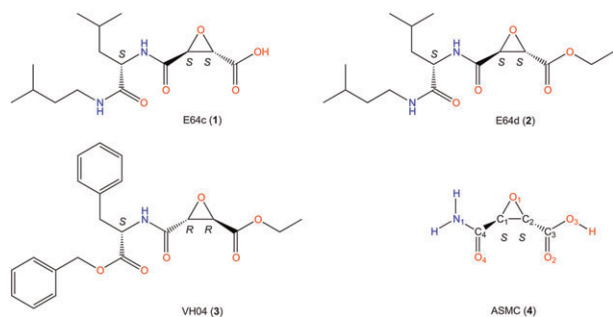
KEYWORDS

electron density, epoxysuccinyl peptides, invarions, model energies, protease inhibitors

1 | INTRODUCTION

Peptides with epoxides as electrophilic building blocks are potent cysteine^[1] and aspartate^[2] protease inhibitors with the epoxysuccinyl peptides being a well-known class of irreversible inhibitors of papain-like cysteine proteases (CAC1 enzymes). Numerous derivatives have been synthesized, all of which derive from the natural product E64 that was

isolated from an *Aspergillus* strain in 1978^[3] and tested against diseases such as muscular dystrophy, osteoporosis, cancer, and Alzheimer over the last 35 years.^[4] In this class of compounds, loxistatin acid (E64c, **1**, Scheme 1) was proven to be one of the most effective inhibitors of enzymes of the papain family.^[5] It is widely used in in-vitro and in-vivo studies.^[6] The ethyl ester loxistatin (E64d, **2**, Scheme 1) is used as a cell-permeable prodrug releasing the



SCHEME 1 Molecular structures of the *trans*-epoxysuccinyl amide compounds investigated in this study. Atom labelling scheme of all compounds according to the active site model compound. For a detailed labelling scheme of all compounds including labels of hydrogen atoms, see the Supporting Information

active acid after hydrolysis. Mechanistic investigations— involving protein crystal structures of E64c-cathepsin B and E64c-papain complexes—show that the inhibition is covalent based on a nucleophilic ring-opening reaction between the epoxide and the active site of the enzyme.^[7] It is irreversible if the epoxide resides in the *S,S* configuration, whereas the inhibition potency is much lower in the *R,R* configuration.^[8]

In general, a covalent inhibition is divided into 2 steps (Figure 1): (1) the formation of a reversible complex of enzyme (E) and inhibitor (I) as a short-lived intermediate (EI) guided by K_i , the dissociation constant of the reversible complex, and (2) the formation of the covalent bond leading to the irreversible complex E-I guided by k_i , the first-order rate constant of the inhibition. The significance of the individual hydrogen bonding network to both steps has been investigated in detail for deprotonated E64c in cathepsin B (Figure 1).^[7e] Only hydrogen bonds from and to the carboxylate and amide groups immediately adjacent to the attacked epoxide ring are of importance, not amide bonds further along the chain. Thus, in this study, we will focus only on the central carboxyl-epoxide-amide motif, which we refer to as the *trans*-epoxysuccinyl amide group.

It has been shown that the conformation of a compound in its crystal structure and inside a biological receptor can

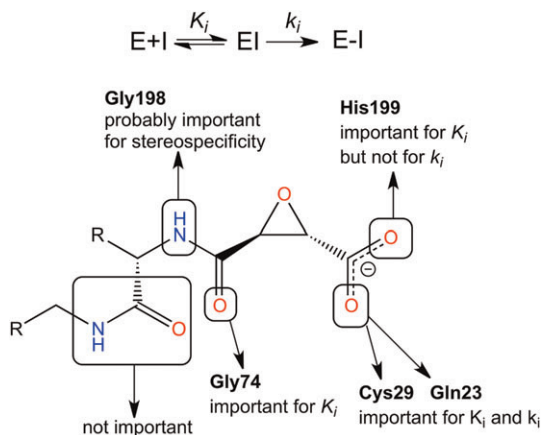


FIGURE 1 Inhibition mechanism and importance of hydrogen bonding in the carboxylate form of E64c^[7e]

be very similar owing to similar forces acting upon the molecule,^[9] namely, electrostatic forces, hydrogen bonding, and van der Waals interactions. In numerous studies, there is a “nearly perfect correlation between small-molecule structural results, and the observed binding in receptor-substrate complexes”.^[9a] From these findings concerning geometry, it can be assumed that the electron density (ED) of the low-molecular weight inhibitor in its pure crystal structure is similar to its ED in the enzyme pocket. This enhances the significance of experimental ED determinations of small biologically active compounds.^[10,11] The presence of ligand-specific induced-fit mechanisms or significant solvation phenomena might limit the applicability of this approach. This aspect and its effect on the ED distribution of the epoxide ring in E64c and E64d were previously investigated by theoretical computations.^[12]

In the past, experimental ED studies were only possible using epoxide-containing compounds with a different substitution pattern,^[13] ie, not containing the biologically intrinsically important epoxysuccinyl amide group (c.f. Figure 1). However, with our recent crystal structure elucidation of E64c^[14] and the overwhelming similarity between the conformation and hydrogen bonding pattern in this crystal structure and those of E64c in the cathepsin B complex, the need for an experimental ED study of the *trans*-epoxysuccinyl amide group becomes obvious. Unfortunately, reduced crystal quality and various other problems described by Shi et al.^[14] prevented an experimental ED determination of pure E64c.

In this study, we describe two alternative ways to obtain the ED information of the epoxysuccinyl amide group: (1) synthesis and diffraction experiments of smaller model compounds that include the *trans*-epoxysuccinyl amide group and (2) use of the invariom approach. Invarioms are pseudoatoms constructed of theoretically calculated multipoles from small model compounds using the transferability principle of submolecular properties, herein multipole parameters.^[15] These invarioms are deposited in a database and can be transferred to the molecule under investigation.^[16] The primary aim is to improve the quality of structural information in a refinement using aspherical instead of standard spherical atomic scattering factors. Additionally, these allow the derivation and subsequent analysis of a total aspherical multipole-based ED distribution consistent with the experimental geometry but being of theoretical nature. It has been shown that this invariom-derived ED can give valuable insight into properties of biologically active compounds.^[17] Therefore, we applied the invariom approach to the new crystal structure of E64c and the model compounds synthesized in this work; see next paragraph.

For the synthesis of model compounds bearing the *trans*-epoxysuccinyl amide moiety, we followed two pathways. The first was an exchange of the alkyl chains of E64c—which proved to be the cause of disorder and therefore modelling problems in the crystal structure—with aryl

substituents hoping to obtain better crystal quality and scattering behaviour. We only partially succeeded as the compound with the best scattering behaviour of all those tested, namely, compound **3** (VH04, see Scheme 1), is still affected by disorder in one of the substituents. However, a high-resolution single-crystal X-ray diffraction data set could be measured at the synchrotron beamline 15-ID-B of the Advanced Photon Source, Argonne National Laboratories, United States. With the recent developments in the invariom approach,^[18] this disorder could be modelled successfully and the structure is of high quality despite the disorder. Two aspects that lower the comparability to E64c are the configuration of the epoxide ring and the ester group connected at the carboxyl end that rather resembles E64d. Since the impact of absolute configuration on the ED of the carbon atoms is not detectable anyway, we neglected this point in the following analysis. However, to investigate the influence of the ester group, we included E64d in the study alongside with E64c. We obtained the crystal structure of E64d from Ishida et al.^[19]; however, we did not perform invariom modelling of this structure because structure factors were not published.

In the second synthetic pathway, we focused only on the epoxysuccinyl amide group saturated with hydrogen atoms since the long side chains seem to be the reason for nonoptimal crystal packing. We succeeded in obtaining a small active site model compound (ASMC, **4**, Scheme 1), which resembles E64c in terms of configuration and protonation of the carboxyl group. Again, experimental difficulties prevented an experimental ED study of **4**. We failed to isolate ASMC from the protonation agent and therefore only obtained cocrystals of **4** with potassium trifluoroacetate. These crystals decomposed under ambient conditions and within various oils, so that we could only obtain a medium-resolution structure at 100 K measured at the in-house diffractometer. We therefore applied invarioms to get an improved structure and a high-quality estimate of the experimental ED as well.

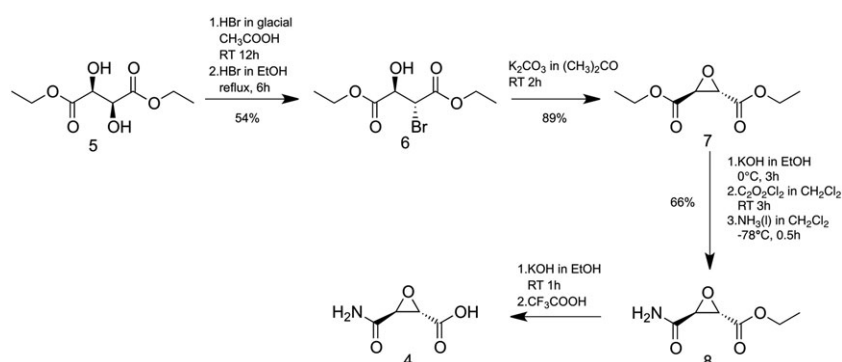
VH04 (**3**) is only weakly active against cysteine proteases (see Section 2.1) as E64d is only weakly active, whereas E64c is, as discussed above, very active. The obvious reasons are the ester group that VH04 has in common

with E64d in contrast to E64c and the wrong absolute configurations of C₁ and C₂ (see above). However, beyond these two known factors, electronic and steric substituent effects as well as the crystal packing will be discussed in Section 3. ASMC (**4**) was not tested for its biological activity, since it only serves as a small model compound to gain access to the ED of the *trans*-epoxysuccinyl amide region. It is not the aim of this study to investigate whether the ED of an inhibitor in a crystal serves as a model for the ED of the inhibitor in the active site. We rather clarify the suitability of ASMC (**4**) as a model along with the requisite alterations to be carried out in future studies to obtain an experimental ED that is most similar to that of E64c. In detail, we will analyse the results for **1** to **4** in two different ways. First, we will compare geometry and ED parameters—derived from invariom refinement (inv) and theoretical isolated-molecule calculations upon geometry optimization (opt)—in the framework of the quantum theory of atoms in molecules (QTAIM)^[20] as well as electrostatic potential (ESP) parameters derived the same way. These parameters are not polarized or perturbed by the environment, so they reflect substituent effects on the *trans*-epoxysuccinyl amide group. Second, we will investigate similarities and differences in the crystal packing with the aid of Hirshfeld surface analysis^[21] and by using model energies^[22] as well as energy framework analysis,^[23] both of which are recent developments within the CrystalExplorer^[24] software.

2 | EXPERIMENTAL SECTION AND COMPUTATIONAL DETAILS

2.1 | Syntheses of model compounds

In Scheme 2, the synthesis of the target compound **4** initially followed a modified procedure of Moriwake et al.^[25] The two-step bromination of (–)-diethyl-D-tartrate proceeds first through hydroxyl acetylation with HBr (33% in glacial acetic acid) followed by dropwise treatment with an excess amount of HBr (33% in glacial acetic acid) in ethanol to afford the brominated succinate in 54%, thereby yielding a single diastereoisomer **6**. Based on the configuration of the starting



SCHEME 2 Synthetic pathway to the active site model compound (ASMC) **4**

material and proposed mechanism by Moriwake et al.,^[25] the product contained the *R,S* configuration. Following the bromination step, the epoxide ring was constructed intramolecularly upon treatment with K_2CO_3 (89% yield). Subsequent hydrolysis of one ester group using a stoichiometric amount of KOH was possible to afford the potassium carboxylate salt. The ensuing carboxylate ion was then converted to its corresponding acid chloride upon treatment with oxalyl chloride. Following the analysis of the crude product, the dried oil was subjected to excess liquid ammonia at $-78^\circ C$ to provide the amide epoxide **8** in 66% yield over 3 steps. The saponification of the ethyl ester **8** was problematic especially given the workup conditions and the susceptibility of the epoxide to ring opening. A stoichiometric amount of pure CF_3COOH appeared to render the protonation possible without any noticeable side reactions; however, removal of the potassium trifluoroacetate was not achieved.^[26] The product **4** cocrystallized with potassium trifluoroacetate and the crystals were also used for 1H nuclear magnetic resonance (NMR) and ^{13}C NMR analyses after dissolving them in appropriate solvents.

Compound **3** (VH04) was synthesized by propylphosphonic anhydride-mediated coupling of *L*-phenylalanyl benzyl ester to the (*R,R*)-configured potassium salt of the enantiomer of compound **8**—which was synthesized according to the (*S,S*)-configured isomer—but starting from (+)-diethyl *L*-tartrate. VH04 was tested regarding its biological activity against cysteine proteases. For inhibition of cathepsins B and L, second-order rate constants of inhibition of 4917 and 72718 $M^{-1} min^{-1}$, respectively, were found, which show that the compound is considerably less active than E64c (298000 $M^{-1} s^{-1}$, cathepsin B; 206000 $M^{-1} s^{-1}$, cathepsin L^[27]).

2.2 | X-ray data collection and data treatment

Details on measurement and data treatment for E64c^[14] and E64d^[19] are given in the original literature. The data set of VH04 (**3**) was measured at synchrotron beamline 15-ID-B of the Advanced Photon Source of the Argonne National Laboratories, United States, equipped with a Bruker Apex 2 CCD area detector using a wavelength of 0.41328 Å and a temperature of 12 K maintained through an open-flow helium-cooling device. 121 054 reflections were collected up to a resolution of 0.48 Å (around 95% completeness), reduced to 10 197 unique reflections in the orthorhombic space group $P2_12_12_1$. No absorption correction was deemed necessary with $\mu = 0.097 mm^{-1}$. The *R* value after spherical refinement was 4.63%. After invariom treatment, the *R* value improved to 3.76%.

Measurements for compounds **4** and **8** were performed on the in-house Oxford Diffraction Xcalibur and Gemini diffractometers, fitted with conventional graphite-monochromated $Mo-K_\alpha$ radiation sources. Measurements were conducted at 100 K. For compound **4**, 36611

reflections were collected up to a resolution of 0.60 Å (around 100% completeness), reduced to 2701 unique reflections in the orthorhombic space group $C222_1$. A multiscan absorption correction was carried out. The *R* value after spherical refinement was 2.57%. After invariom treatment, the *R* value improved to 2.51%.

For all compounds **1**, **3**, **4**, and **8**, pertinent details are given in Table S1 (Supporting Information) and the crystallographic information files are deposited with the Cambridge Database. They can be obtained free of charge under <https://summary.ccdc.cam.ac.uk/structure-summary-form>. The Cambridge Crystallographic Data Centre deposition numbers are 977799 and 1498219 to 1498221.

All structures were solved with SHELXS^[28] using direct methods and initially refined against F^2 , using full-matrix least squares methods, with the program SHELXL^[28] within SHELXL^[29]. Compounds **1**, **3**, and **4** were subsequently treated with the program InvariomTool^[16] for the invariom transfer and XD2006^[30] for the refinement using the fixed theoretical multipoles from the invariom databank. XDPROP was used for the topological ED analysis and XDGRAPH for the generation of maps. The program MOLISO^[31] was used for generating the representations of the ESP mapped onto Hirshfeld surfaces. The program CrystalExplorer^[24] was used for Hirshfeld surface analyses, calculation of interaction energies, and generation of energy framework representations.

2.3 | Quantum chemical calculations

Isolated-molecule geometry optimizations for E64c (**1**), E64d (**2**), VH04 (**3**), and ASMC (**4**) were performed with the program Gaussian09^[32] at the B3LYP/6-311++G(2d,2p) level of theory. Subsequent frequency analyses confirmed that the obtained geometries were minima on the potential energy hypersurface. The topological analysis of the ED was carried out with the program AIM2000.^[33]

CrystalExplorer model energies were calculated according to the procedure described by Turner et al.^[22] Therein, the total energy is the sum of four scaled energy components (electrostatic, polarization, repulsion, and dispersion energies). The scale factors are derived from a fit to counterpoise- and dispersion-corrected density functional theory energies for a large set of neutral molecular dimers at the B3LYP-D2/6-31G(d,p) level of theory. Therefore, the model energies for compounds **1** to **4** in this paper are based on monomer calculations (with Gaussian as interfaced with CrystalExplorer) at the B3LYP/6-31G(d,p) level, which is the default setting in CrystalExplorer. Note that the individual energy components as given in Table 5 are not scaled; the scale factors are only used in the calculation of the total energy. Moreover, for pairwise interactions involving ions, the same methodology is applied but is neither benchmarked nor tested. The results occur to be meaningful but have to be treated with care.

3 | RESULTS AND DISCUSSION

3.1 | Intramolecular geometry and electron density

The experimental bond lengths and angles of the *trans*-epoxysuccinyl amide region in compounds **1** to **4** are reported in Table 1. Although the crystal structure of **1** has four symmetry-independent molecules in the asymmetric unit, an earlier study has shown that the major structural deviations occur at the terminal alkyl group.^[14] Hence, the active sites or backbones of the four E64c molecules have similar geometries; in fact, the bond lengths and angles agree with each other mostly within the experimental uncertainties (see Supporting Information). Therefore, in Table 1 and in the following analyses, one of the nondisordered E64c molecules in the asymmetric unit (molecule D) is used as the representative example of **1** for comparison with compounds **2**, **3**, and **4**. The experimental bond lengths and angles within the epoxide ring of the four compounds exhibit only minor variation. The C₁–O₁–C₂ angle is around 4° larger than the two O–C–C angles, which is consistent with values found for different biologically active epoxides.^[13] In compound **4**, the epoxide is closest to an equilateral triangle. The only significant bond

angle deviation is O₁–C₁–C₄ in **4** being 3° to 4° smaller than the same angle in the other compounds, all of which bear large substituents at amide nitrogen atom N₁ in contrast to **4**. This difference is reflected in the C₁–C₄ bond lengths, but not in the C₄–N₁ bond lengths. C₁–C₄ is longer by about 0.02 Å compared with **1** to **3**. In summary, in terms of geometry, the small model compound **4** is the only one that shows differences in the active region.

To indicate whether the described differences are caused by substituent effects or crystal packing, we additionally listed in Table 1 the geometrical parameters obtained from isolated-molecule geometry optimization. The theoretical calculations even out the differences; see, e.g., the C₁–C₄ bond distances that are now around 1.514 Å for all compounds. This indicates that it is not substituent effects that are responsible for the geometrical differences in the active region, but the crystal packing (see Section 3.2). Whether or not substituent effects have an influence on the ED distribution of the active region will be discussed in the following paragraphs.

The shape of the aspherical valence ED distribution in the relevant *trans*-epoxysuccinyl amide is depicted in Figure 2 based on invariom transfer for E64c. Since the invarioms used in this region are identical for all compounds **1**, **3**, and **4**, the maps for the other compounds look virtually identical (shown in the Supporting Information); only the atomic positions vary slightly after refinement (see Table 1). The ED around C₄–O₄ in the amide group (Figure 2A) is very similar to that around C₃–O₂ in the carboxyl group (Figure 2B) with 2 pronounced oxygen lone pairs in the plane. N₁ and O₃ differ in terms of the negative deformation density around O₃ in Figure 2B, which is not present around N₁. This indicates more covalency for C–N bonds or more ionicity for C–O bonds; see the bond-critical point (BCP) properties in Table 2, especially the more negative Laplacian value for C–N bonds compared with C–O bonds in the opt model (the inv model is not reliable for C–O bonds, see below). However, N₁ and O₃ have in common that their lone pairs extend perpendicularly to the plane in contrast to those of O₄ (so the lone pair of N₁ cannot be seen in this plane). The lone pairs of these 4 atoms (O₂, O₃, O₄, and N₁) are important for forming the biologically relevant hydrogen bonds (see Figure 1). The epoxide oxygen O₁ is not involved in any interactions of importance (Figure 1), and its two lone pairs (Figure 2C, also extending perpendicularly to the plane) are less pronounced and do not reach as far as the oxygen lone pairs in the amide or carboxyl groups. Note that the shapes of these lone pairs are unperturbed by the environment, so they represent the situation before interactions are formed.

Moreover, it is evident that the shapes of the C–C and C–O deformation densities in the epoxide ring are significantly different from the shapes of C–C and C–O bonds in the amide or carboxyl groups, indicating a bent (or banana-shaped) bond. This is consistent with the high ellipticity values at the BCPs assembled in Table 2, and with previous

TABLE 1 Geometries of the *trans*-epoxysuccinyl amide region of compounds **1** to **4**

	E64c (1)	E64d (2)	VH04 (3)	ASMC (4)
C ₁ –C ₂	1.473(8) 1.479	1.468(5) 1.478	1.480(1) 1.478	1.472(2) 1.479
C ₁ –O ₁	1.421(6) 1.420	1.422(4) 1.421	1.423(1) 1.419	1.428(2) 1.418
C ₂ –O ₁	1.420(8) 1.419	1.420(5) 1.421	1.417(1) 1.423	1.425(2) 1.420
C ₂ –C ₃	1.497(9) 1.500	1.491(6) 1.504	1.497(1) 1.504	1.502(2) 1.501
C ₃ –O ₂	1.216(9) 1.201	1.201(5) 1.204	1.203(1) 1.207	1.215(2) 1.201
C ₃ –O ₃	1.308(8) 1.353	1.313(6) 1.344	1.331(1) 1.340	1.305(2) 1.351
C ₁ –C ₄	1.495(8) 1.514	1.507(4) 1.514	1.503(1) 1.514	1.521(2) 1.515
C ₄ –N ₁	1.344(6) 1.356	1.330(4) 1.357	1.341(1) 1.366	1.338(2) 1.362
C ₄ –O ₄	1.231(7) 1.220	1.218(4) 1.220	1.231(1) 1.216	1.228(2) 1.213
C ₁ –O ₁ –C ₂	62.5(4) 62.8	62.2(2) 62.7	62.8(1) 62.7	62.1(1) 62.8
O ₁ –C ₁ –C ₂	58.7(4) 58.6	58.8(2) 58.7	58.4(1) 58.8	58.8(1) 58.6
O ₁ –C ₂ –C ₁	58.8(4) 58.6	59.0(2) 58.6	58.8(1) 58.5	59.0(1) 58.6
O ₁ –C ₂ –C ₃	116.8(6) 116.1	115.5(3) 116.0	117.7(1) 116.3	115.0(1) 115.9
O ₁ –C ₁ –C ₄	117.4(5) 116.3	115.9(3) 116.2	117.0(1) 116.6	112.8(1) 116.2

Distances in Å, angles in degrees. See Scheme 1 for atom numbering. First row: experimental values (invariom derived for **1**, **3**, and **4**; from Ishida et al.^[19] for **2**); second row: optimized geometry. For **1**, disorder-free molecule D in the asymmetric unit is used.

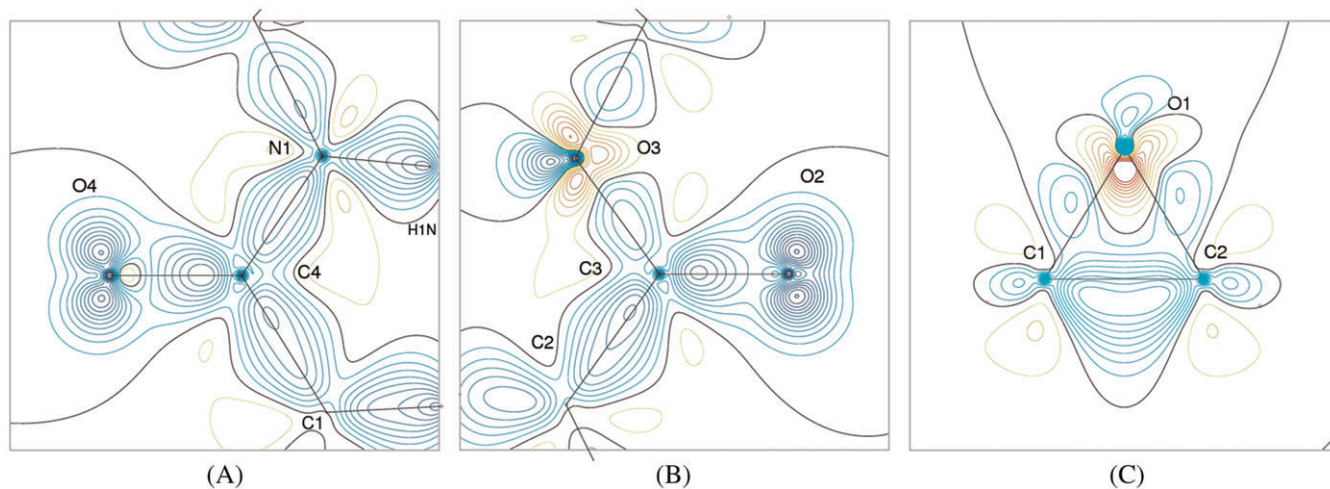


FIGURE 2 Static deformation density maps of the *trans*-epoxysuccinyl amide group in E64c (**1**) after invariom refinement. (A), Amide group (atoms defining the plane: O₄, C₄, and N₁). (B), Carboxylate group (O₃, C₃, and O₂). (C), Epoxide ring (O₁, C₁, and C₂). Contour interval: 0.1 eÅ⁻³ for A and B and 0.05 eÅ⁻³ for C

TABLE 2 Bond-topological properties at the bond-critical points of the *trans*-epoxysuccinyl amide group of compounds **1** to **4** from invariom refinement (inv) and after isolated-molecule geometry optimization (opt)

		ρ		$\nabla^2\rho$		ϵ	
		inv	opt	inv	opt	inv	opt
C ₁ –C ₂	E64c (1)	1.739	1.655	-8.61	-11.25	0.46	0.31
	E64d (2)	N/A	1.663	N/A	-11.45	N/A	0.3
	VH04 (3)	1.688	1.661	-7.78	-11.39	0.45	0.3
	ASMC (4)	1.709	1.656	-8.30	-11.27	0.42	0.31
C ₁ –O ₁	E64c (1)	1.814	1.752	-6.78	-12.04	0.54	0.44
	E64d (2)	N/A	1.747	N/A	-11.93	N/A	0.46
	VH04 (3)	1.750	1.753	-5.18	-12.02	0.52	0.45
	ASMC (4)	1.734	1.758	-4.77	-12.15	0.53	0.44
C ₂ –O ₁	E64c (1)	1.778	1.755	-5.44	-12.14	0.56	0.46
	E64d (2)	N/A	1.744	N/A	-11.88	N/A	0.47
	VH04 (3)	1.753	1.741	-5.05	-11.82	0.51	0.47
	ASMC (4)	1.737	1.752	-4.33	-12.07	0.51	0.46
C ₂ –C ₃	E64c (1)	1.807	1.786	-12.88	-15.54	0.16	0.11
	E64d (2)	N/A	1.776	N/A	-15.29	N/A	0.11
	VH04 (3)	1.868	1.776	-14.71	-15.32	0.17	0.1
	ASMC (4)	1.868	1.784	-14.21	-15.50	0.16	0.11
C ₃ –O ₂	E64c (1)	3.024	2.928	-33.37	-13.68	0.08	0.12
	E64d (2)	N/A	2.906	N/A	-13.67	N/A	0.12
	VH04 (3)	3.026	2.885	-33.34	-14.07	0.08	0.12
	ASMC (4)	2.979	2.927	-33.72	-13.72	0.09	0.12
C ₃ –O ₃	E64c (1)	2.326	2.054	-27.63	-18.37	0.09	0.03
	E64d (2)	N/A	2.096	N/A	-18.27	N/A	0.05
	VH04 (3)	2.210	2.109	-23.18	-18.33	0.12	0.05
	ASMC (4)	2.294	2.062	-26.87	-18.40	0.10	0.03
C ₁ –C ₄	E64c (1)	1.818	1.735	-13.39	-14.41	0.09	0.08
	E64d (2)	N/A	1.738	N/A	-14.46	N/A	0.08
	VH04 (3)	1.803	1.732	-13.54	-14.33	0.13	0.09
	ASMC (4)	1.794	1.754	-13.07	-14.84	0.14	0.09
C ₄ –N ₁	E64c (1)	2.314	2.210	-22.92	-25.36	0.11	0.18
	E64d (2)	N/A	2.205	N/A	-25.28	N/A	0.18
	VH04 (3)	2.315	2.164	-23.00	-24.54	0.23	0.17
	ASMC (4)	2.307	2.175	-22.81	-25.02	0.17	0.15
C ₄ –O ₄	E64c (1)	2.858	2.808	-31.90	-16.46	0.09	0.1
	E64d (2)	N/A	2.806	N/A	-16.48	N/A	0.1
	VH04 (3)	2.874	2.835	-32.29	-16.10	0.09	0.11
	ASMC (4)	2.897	2.853	-33.50	-15.79	0.09	0.11

Electron density (ρ in eÅ⁻³), Laplacian of electron density ($\nabla^2\rho$ in eÅ⁻⁵), and ellipticity (ϵ). N/A: Invariom refinement of E64d is not available, see Section 1.

experimental ED findings for epoxides.^[13,34] However, it was shown that the corresponding C–O bond paths for epoxides according to the QTAIM are not outward bent, but S-shaped.^[35] The invariom-derived bond paths are consistent with this finding (see Supporting Information for molecular graphs of ASMC).

Differences between the invariom (inv) and isolated-molecule (opt) models in Table 2 are most striking for the carbonyl C=O bonds (C₃–O₂, C₃–O₃, and C₄–O₄), with the absolute value of the Laplacian at the BCPs being too large by about 10–20 eÅ⁻⁵ in the inv model. This is a known effect for carbonyl bonds—or polar bonds in general—and is due to the inflexibility of the radial functions in the multipole formalism that is the basis for invariom treatment.^[12b,36] To avoid these significant inconsistencies, we must improve or replace the underlying multipole model itself. Efforts towards this goal are on the way by several groups,^[37] including our own group.^[38] However, for problematic structures, such as the disordered E64c and VH04 structures, the invariom model is currently—aside from similar pseudoatom database techniques^[39]—the only practical and successful way of obtaining a useful ED estimate for the crystallographic experiment and a reliable high-quality experimental structure. It is noteworthy, though, that for the C–O bonds in the epoxide ring (C₁–O₁ and C₂–O₁) and the C₄–N₁ bond, the absolute value of the Laplacian at the BCPs is slightly smaller in the inv model than in the opt model. However, for the purpose of identifying possible substituent effects in the ED properties, only the bond-topological properties from the opt model will be discussed, and atomic properties integrated over the atomic basin (Table 3) that are far less susceptible to model problems than properties at the BCPs.

From the BCP properties (opt model, Table 2), substituent effects are very hard to identify because the values are quite similar between the different compounds **1** to **4**.

TABLE 3 Atomic properties of the *trans*-epoxysuccinyl amide group of compounds **1** to **4** from invariom refinement (inv) and after isolated-molecule geometry optimization (opt)

		Q		V	
		inv	opt	inv	opt
O ₁	E64c (1)	-0.80	-0.82	15.50	16.17
	E64d (2)	N/A	-0.82	N/A	16.20
	VH04 (3)	-0.79	-0.81	14.35	16.17
	ASMC (4)	-0.75	-0.81	13.76	16.14
O ₂	E64c (1)	-0.94	-1.09	16.44	20.01
	E64d (2)	N/A	-1.09	N/A	19.53
	VH04 (3)	-0.95	-1.12	17.30	19.65
	ASMC (4)	-0.87	-1.09	17.01	19.99
O ₃	E64c (1)	-1.08	-1.04	16.79	18.03
	E64d (2)	N/A	-1.02	N/A	14.96
	VH04 (3)	-0.96	-1.01	14.20	14.88
	ASMC (4)	-1.06	-1.04	15.88	18.00
O ₄	E64c (1)	-0.91	-1.11	16.28	19.51
	E64d (2)	N/A	-1.11	N/A	19.53
	VH04 (3)	-0.92	-1.08	15.05	20.06
	ASMC (4)	-0.92	-1.08	18.92	20.11
N ₁	E64c (1)	-0.97	-1.01	12.01	13.15
	E64d (2)	N/A	-1.01	N/A	13.15
	VH04 (3)	-0.98	-0.98	11.94	13.15
	ASMC (4)	-0.91	-1.00	16.67	17.12
C ₁	E64c (1)	0.27	0.39	8.43	8.27
	E64d (2)	N/A	0.39	N/A	8.27
	VH04 (3)	0.24	0.38	8.21	8.12
	ASMC (4)	0.23	0.39	8.49	8.28
C ₂	E64c (1)	0.26	0.40	8.72	8.25
	E64d (2)	N/A	0.40	N/A	8.23
	VH04 (3)	0.25	0.40	8.52	8.22
	ASMC (4)	0.26	0.40	8.58	8.24
C ₃	E64c (1)	1.33	1.54	6.28	5.53
	E64d (2)	N/A	1.54	N/A	5.52
	VH04 (3)	1.28	1.54	5.98	5.53
	ASMC (4)	1.28	1.54	5.95	5.52
C ₄	E64c (1)	1.08	1.37	6.93	5.90
	E64d (2)	N/A	1.37	N/A	5.90
	VH04 (3)	1.09	1.37	6.28	5.90
	ASMC (4)	1.15	1.39	7.27	5.85

Charge (Q in e) and volume (V in Å³) were cut at an electron density isovalue of 0.001 a.u.. For N/A, see footnote to Table 2.

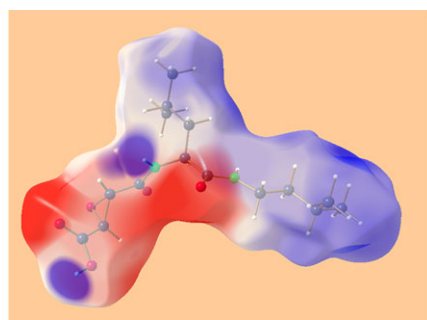
Especially for the bonds C₄-N₁ and C₃-O₃, which are directly adjacent to the variable substituents, no trend can be found. Since it is known that in the biological inhibition process the C₂ atom in E64c is attacked under cleavage of the C₂-O₁ bond (c.f. Section 1), a comparison between C₁-O₁ and C₂-O₁ is interesting. However, neither in E64c nor in ASMC can C₂-O₁ be identified to be more labile than C₁-O₁. Hence, the enzyme function, or more generally speaking environmental effects, must play a crucial role in preparing the inhibition reaction (c.f. reaction mechanism in Figure 1 and discussion in Section 1). Therefore, a detailed analysis of the crystal packing that can mimic the biological environment as a first approximation is crucial; see Section 3.2.

The atomic charges on atoms C₁ and C₂ (Table 3) are nearly identical for E64c, and only in the inv model of ASMC (**4**) is C₂ slightly more positively charged than C₁ and simultaneously of a higher volume, favouring a nucleophilic attack at C₂. In addition, C₃ and C₄ in the amide or carboxyl groups

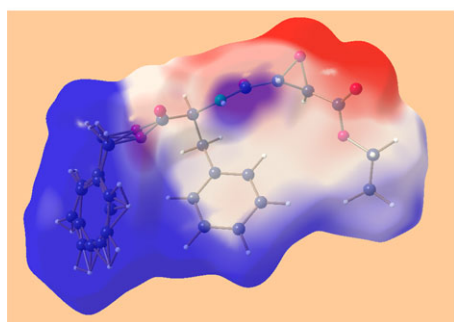
are much more positively charged than C₁ and C₂, so that the atomic charges alone cannot explain the reactivity of the active site. On the other hand, C₁ and C₂ are significantly larger in volume than C₃ and C₄. In summary, the environment and not the inherent electronic properties must be decisive for the mechanism of the inhibition reaction. This is corroborated by the fact that no significant or meaningful differences can be found between E64c, E64d and VH04 (in neither bond-topological nor atomic properties, Tables 2 and 3) that would explain the different biological activities. Oxygen atom O₁ in the epoxide ring is less negatively charged than all other oxygen atoms, and the nitrogen atom N₁ is charged about the same as the oxygen atoms. All heteroatoms except O₁ in E64c are involved in hydrogen bonds that influence the reaction mechanism of the inhibition. It is interesting that for N₁ a substituent effect can be observed in ASMC (**4**), with N₁ only bearing hydrogen atoms compared with compounds **1** to **3** in which N₁ carries one bulky substituent and one hydrogen atom. The charge of N₁ in **4** is slightly lower in the inv model and its volume significantly bigger. The charge difference is evened out in the isolated-molecule calculations, but the volume difference is preserved. Likewise, a substituent effect can be observed for O₃ that is more negatively charged and bigger in both models inv and opt for the acids E64c (**1**) and ASMC (**4**) compared with the esters E64d (**2**) and VH04 (**3**). However, these effects on N₁ and O₃ are not propagated to other atoms further inside the *trans*-epoxysuccinyl amide moiety.

Figure 3 displays the invariom-generated ESPs mapped onto their Hirshfeld surfaces.^[40] Neither invarioms nor Hirshfeld surfaces are influenced by crystal packing effects (polarization)—only indirectly through geometry differences caused by crystal packing; hence, Figure 3 does not represent a way of depicting intermolecular interactions, but the inherent electrostatic properties of the underlying molecules before they are polarized by their neighbours in the crystal. Since it has been shown previously that invarioms offer a quick and reliable access to ESPs of biologically active molecules^[41] and since an invariom refinement has not been possible for **2** (see Section 1), we only discuss the ESPs of **1**, **3**, and **4**. A comparison between the ESPs of E64c (**1**) and E64d (**2**) derived from isolated-molecule calculations can be found in the Supporting Information.

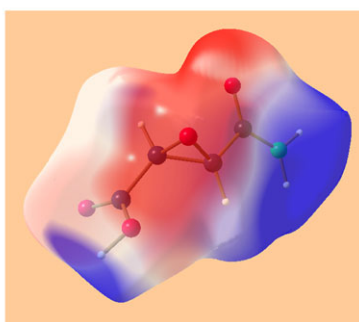
The first obvious (nonelectronic) substituent effect is the shape of the Hirshfeld surface. It visualizes the steric differences of the molecules. Although Scheme 1 might suggest that E64c and VH04 are similar in size, the shape of their molecular surfaces is significantly different—even if the disorder in VH04 is disregarded—with E64c being more T-shaped and VH04 being more rectangular. The distribution of positive and negative regions of the ESP on the Hirshfeld surfaces according to the underlying atoms is not surprising. However, a clear difference can be found by generating the ESP distribution statistics on the Hirshfeld surface according to Politzer.^[42,43] The parameter Π , the average deviation from



(A)



(B)



(C)

FIGURE 3 Invariom-generated electrostatic potentials mapped onto Hirshfeld surfaces of (A) E64c (**1**), (B) VH04 (**3**), and (C) ASMC (**4**). Colour code: $-0.1 \text{ e}\text{\AA}^{-1}$ (red), $0 \text{ e}\text{\AA}^{-1}$ (white), $+0.1 \text{ e}\text{\AA}^{-1}$ (blue)

the mean surface potential, the so-called internal charge separation or local polarity, has been used before to be

TABLE 4 Hydrogen bond geometries based on invariom refinement of compounds **1**, **3**, and **4** or based on the published structure for **2**, respectively, including short potassium carboxyl contacts in **4**

CPD		D–H (Å)	H–A (Å)	D...A (Å)	D–H...A (°)	Symmetry ^a	
E64c (1)	O ₃ D–H ₁ AD...O ₅ C	0.962(12)	1.593(10)	2.539(7)	166.6(8)	Intra asu	
	N ₁ D–H ₁ BD...O ₂ C	1.014(12)	1.830(11)	2.828(8)	167.0(8)	Intra asu	
	N ₂ D–H ₁ CD...O ₄ B ^a	1.000(11)	1.911(11)	2.879(7)	162.1(9)	$x, y, 1 + z$	
	C ₁ D–H ₁ DD...O ₂ C	1.084(12)	2.504(12)	3.291(9)	128.6(9)	Intra asu	
	O ₅ D...H ₁ AC–O ₃ C	0.959(12)	1.635(10)	2.555(8)	159.5(8)	Intra asu	
	O ₂ D...H ₁ BC–N ₁ C	1.000(11)	1.873(12)	2.831(8)	159.5(7)	Intra asu	
	O ₄ D...H ₁ CB ^a –N ₂ B ^a	1.010(9)	1.980(11)	2.934(9)	156.5(8)	$-1 + x, y, 1 + z$	
	O ₂ D...H ₁ DC–C ₁ C	1.077(11)	2.533(12)	3.277(8)	125.5(9)	Intra asu	
	E64d (2)	N ₁ –H ₁ N...O ₄ ^a	0.98(4)	1.97(4)	2.941(4)	168(3)	$1 + x, y, z$
		N ₂ –H ₂ N...O ₅ ^a	0.82(3)	2.09(3)	2.909(4)	174(4)	$-1 + x, y, z$
C ₁ –H ₁ ...O ₄ ^a		1.15(4)	2.23(4)	3.331(4)	159(2)	$1 + x, y, z$	
C ₁₆ –H ₁₆ A...O ₁ ^a		1.10(3)	2.56(3)	3.407(6)	133(3)	$1/2 + x, 1/2 - y, 1 - z$	
C ₁₆ –H ₁₆ A...O ₂		1.10(3)	2.58(4)	3.371(6)	128(3)	Intramolecular	
VH04 (3)		N ₁ –H ₁ N...O ₄ ^a	1.006(1)	2.140(1)	3.112(1)	161.9(1)	$-1 + x, y, z$
	C ₁ –H ₁ ...O ₄ ^a	1.081(1)	2.312(1)	3.253(1)	145.2(1)	$-1 + x, y, z$	
	C ₅ –H ₅ ...O ₅ ^a	1.101(1)	2.172(1)	3.139(1)	145.1(1)	$1 + x, y, z$	
	C ₂₁ –H ₂₁ B...O ₂ ^a	1.096(1)	2.518(1)	3.343(1)	127.0(1)	$1/2 + x, 3/2 - y, 2 - z$	
	C ₂₁ –H ₂₁ B...O ₁ ^a	1.096(1)	2.577(1)	3.395(1)	137.1(1)	$-1/2 + x, 3/2 - y, 2 - z$	
ASMC (4)	O ₃ –H ₂ O...O ₅ ^a	0.961(1)	1.553(1)	2.511(1)	174.4(1)	$1 - x, y, 1/2 - z$	
	N ₁ –H ₁ NA...O ₆ ^a	1.016(2)	2.249(2)	3.009(1)	130.5(1)	$-1 + x, y, z$	
	N ₁ –H ₁ NA...O ₂ ^a	1.016(2)	2.509(2)	3.372(2)	142.5(1)	$-1/2 + x, -1/2 + y, z$	
	N ₁ –H ₁ NB...O ₁ ^a	1.016(2)	2.024(1)	2.972(1)	154.4(1)	$-1/2 + x, 3/2 - y, -z$	
	N ₁ –H ₁ NB...O ₄ ^a	1.016(2)	2.493(1)	3.243(1)	130.2(1)	$-1/2 + x, 3/2 - y, -z$	
	O ₂ ...K ₁ ^a	N/A	N/A	2.761(1)	N/A	$-1/2 + x, 1/2 + y, z$	
	O ₄ ...K ₁ ^a	N/A	N/A	2.854(1)	N/A	$-1/2 + x, 3/2 - y, -z$	
	O ₁ ...K ₁	N/A	N/A	2.928(1)	N/A	Intra asu	
	O ₃ ...K ₁	N/A	N/A	2.933(1)	N/A	Intra asu	
	O ₂ ...K ₁ ^a	N/A	N/A	3.166(1)	N/A	$1/2 - x, 1/2 + y, 1/2 - z$	

For E64c (**1**), only hydrogen bonds involving disorder-free molecule D of the asymmetric unit (asu) are shown. All other symmetry-independent molecules A, B, and C exhibit a very similar hydrogen bonding pattern. Hydrogen bonds in the molecule D that serves as a donor are listed above the dotted line and those in the molecule D that serves as an acceptor are listed below. In **2** and **3** with one molecule per asu, the same molecule serves as a donor and acceptor (symmetric fingerprint plots in Figure 5B and C). Weak C–H...O hydrogen bonds in **3** that involve disordered components are omitted. In **4**, ASMC interacts with itself as an acceptor (O₁) and with cocrystallized potassium trifluoroacetate (K₁, O₅, and O₆); see the Supporting Information (interactions in this crystal structure that do not involve ASMC are omitted, see deposited crystallographic information file for more details). D, donor atom; H, hydrogen atom; A, acceptor atom. H atoms were freely refined. Arbitrary criteria for listing hydrogen bonds are $d(\text{D}...A) < 3.50 \text{ \AA}$, $\angle(\text{D}...A) > 120^\circ$. For a detailed labelling scheme of all compounds including labels of hydrogen atoms, see Supporting Information.

^aSymmetry operations refer to the atoms labelled with a.

correlated to biological activity.^[13,43] In the work of Schneider et al.,^[43] values of Π around $0.050 \text{ e}\text{\AA}^{-1}$ with a spread of approximately $0.003 \text{ e}\text{\AA}^{-1}$ are reported for nine different vinyl sulfone-based cysteine protease inhibitors. Here, we find values of $0.095 \text{ e}\text{\AA}^{-1}$ for VH04 (**3**) and $0.100 \text{ e}\text{\AA}^{-1}$ for ASMC (**4**), whereas the value for E64c (**1**)—the only biologically active cysteine protease inhibitor among **1**, **3**, and **4**—is significantly different and resembles the values found for the vinyl sulfone-based inhibitors ($\Pi = 0.067 \text{ e}\text{\AA}^{-1}$). Hence, Π is the only indicator found so far that shows that the inherent unperturbed electronic distribution might have an influence on the inhibition reaction mechanism in terms of a less extreme distribution of ESP values on the molecular surface as it is felt by neighbours, e.g., the enzyme, in the recognition step (c.f. formation of the reversible complex E-I in Figure 1) before bonds are formed.

3.2 | Crystal packing

In Section 3.1, it has become clear that for understanding the functionality of the *trans*-epoxysuccinyl amide group—and possibly the differences between compounds **1** to **4**—it is crucial to study the intermolecular interactions they are involved in. For the reasons discussed above, we have no access to the experimental ED distribution that would include these intermolecular packing effects. We decided not to carry out theoretical periodic boundary or quantum mechanics/molecular mechanics calculations in this study, but to compare the results of those calculations with the experimental ED once we have managed to obtain it in future studies. Here, we follow a much easier and much more straightforward strategy to gain a detailed insight into crystal packing,

namely, a Hirshfeld surface analysis,^[21] which is purely geometry based, and a model energy^[22] and energy framework analysis,^[23] which have only recently been included into the software CrystalExplorer.^[24] Hence, it is beyond the scope of the present study to determine the crystal packing effect on the ED distribution.

Table 4 lists the hydrogen bonds and close contacts found in compounds **1** to **4**. As discussed in Section 1, it is known that inhibition-relevant hydrogen bonds in E64c exclusively involve atoms from the *trans*-epoxysuccinyl amide region excluding the epoxide oxygen atom O_1 and excluding amide or ester groups further along the chain (see Figure 1 and compare discussion of the lone pairs in Section 3.1). Therefore, we are specifically interested in the existence of those hydrogen bonds in the crystal structures of E64d (**2**) and the other two model compounds (**3** and **4**), keeping in mind that the hydrogen bond pattern in the crystal structure of neutral E64c (ie, not deprotonated at the carboxyl end) is almost identical to that in the cathepsin B-E64c complex (with E64c being deprotonated to a carboxylate), as discussed in detail by Shi et al.^[14] The same donor and acceptor atoms are used for interactions in ASMC (**4**) that are also available in E64c (**1**), namely, $O_3\text{--}H_2O/H_1A$ and $N_1\text{--}H_1$ as donors and O_2 and O_4 as acceptors (neither O_3 and N_1 as acceptors, but additionally O_1 in **4**), and the distances of these interactions are similar (Table 4). Both esters E64d (**2**) and VH04 (**3**) cannot form an $O_3\text{--}H$ hydrogen bond, whereas they both form the same $N_1\text{--}H_1N\dots O_4$ and $C_1\text{--}H_1\dots O_4$ interactions. Hirshfeld surface analysis (Figure 4) confirms that the esters **2** and **3** are similar to each other and different from E64c (**1**) in terms of intermolecular interactions with the closest neighbours: in E64c (**1**), dimers are stabilized by various

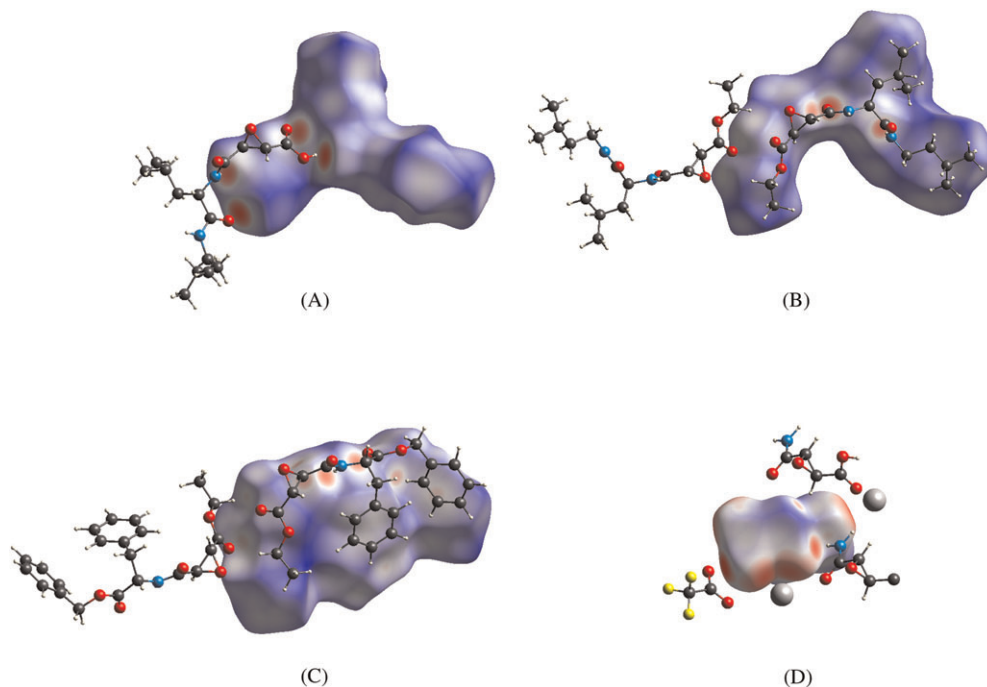


FIGURE 4 Hirshfeld surfaces with the property d_{norm} mapped onto them. (A), E64c (**1**) (molecule D of the asymmetric unit); (B), E64d (**2**); (C), VH04 (**3**) (main disorder component); (D), ASMC (**4**). Colour code of d_{norm} : red = -0.699 , white = 0 , blue = 1.739 . Red regions indicate close contacts

strong hydrogen bonds in a sideways approach (see Figure 4 a), whereas **2** and **3** only exhibit weak interactions with the next side-on partner, but strong interactions with a partner covering the full length of the Hirshfeld surface (compare Figure 4B with Figure 4C). The unpolarized invariom ESP of ASMC (**4**) on its Hirshfeld surface is not more extreme or strikingly different to that of the other compounds (see Figure 3), but, in the cocrystal with ions, strong electrostatic forces act upon ASMC. The ions dominate large areas of the Hirshfeld surface (c.f. Figure 4D), so that a comparison with **1** to **3** is difficult. However, the importance of the carboxyl group in **4** is illustrated by the discussion on model energies below, where the electrostatic forces are quantified.

The fingerprint plots (Figure 5) show that the existence of the O₃-H donor group in the carboxyl functionality of **1** and **4** leads to pronounced spikes representing the hydrogen bonds in both compounds (compare Figure 5A with Figure 5D; the total area of the Hirshfeld surface that is covered by O...H contacts is 38.4% in E64c (**1**) and 39.4% in ASMC (**4**)). In contrast, in the esters E64d (**2**) and VH04

(**3**), hydrogen bonds are more distant (shorter spikes), and the total coverage by O...H contacts is reduced (28.6% for E64d; 29.6% for VH04). The central spike (or the two central spikes) in all fingerprint plots is caused by H...H contacts. In E64c (**1**) and E64d (**2**), they mirror hydrophobic interactions in the alkyl chains (total coverage 57.2% in **1** and 65.6% in **2**). H...H contacts are reduced to 48.4% in VH04 (**3**) because C-H... π interactions (represented by C...H contacts, coverage 17.9%; only 2-3% in **1** and **2**) become important. In ASMC (**4**), a further reduction of H...H contacts is evident (11.2%), and instead K...O, F...O, O...O, and F...C interactions have values between 5% and 12%.

In Table 5, pairwise interactions with their model energies calculated according to Turner et al.^[22] are listed. Through the last column, a connection between pairwise molecular interactions and the classical picture of atom-atom interactions (Table 4) is drawn. The only pairwise interactions where the electrostatic component is large and negative—here, below -10 kJ mol^{-1} for all four investigated compounds—are those where hydrogen bonds and O...K

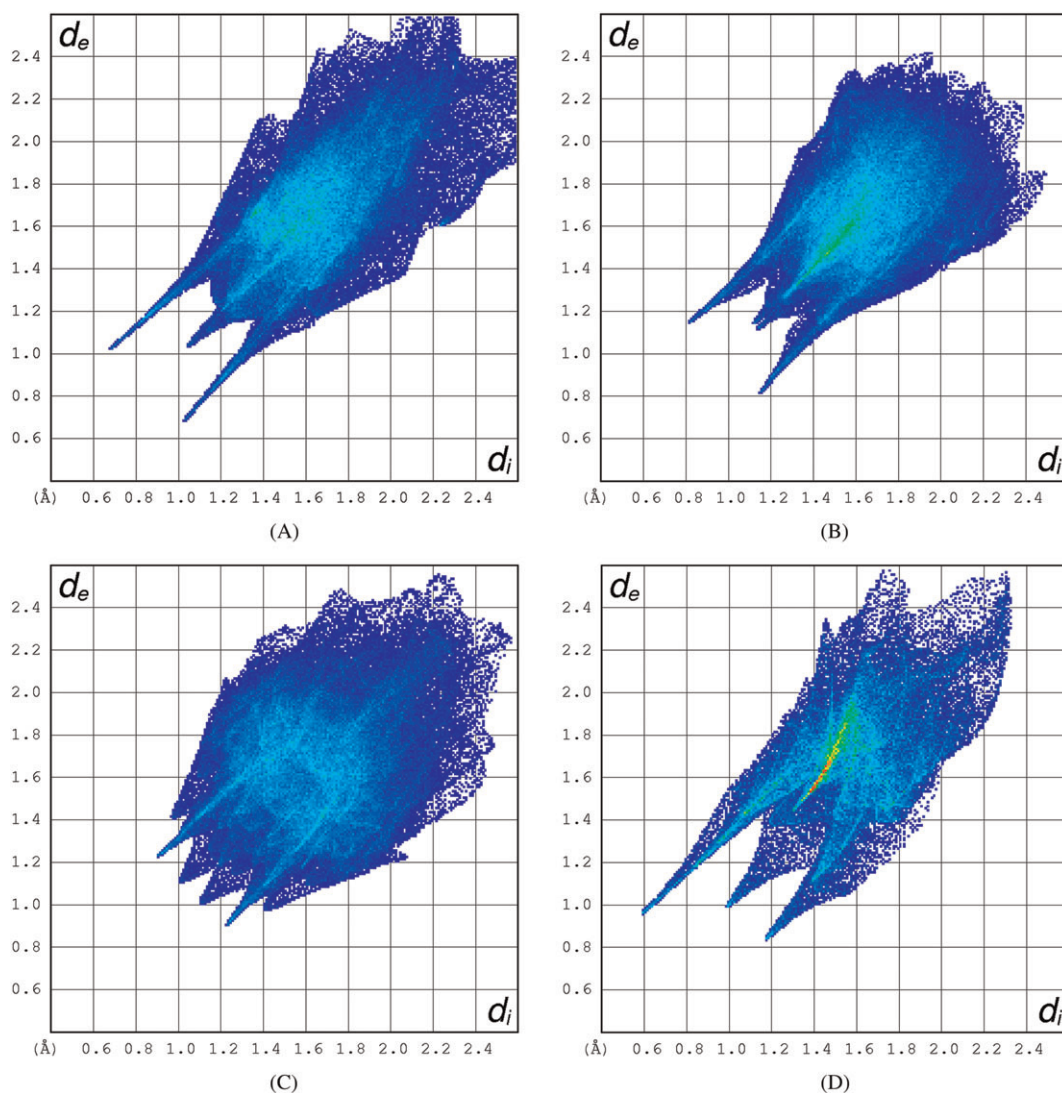


FIGURE 5 Hirshfeld surface fingerprint plots of (A) E64c (**1**) (molecule D of the asymmetric unit), (B) E64d (**2**), (C) VH04 (**3**) (main disorder component), (D) ASMC (**4**)

TABLE 5 CrystalExplorer model energies (kJ mol⁻¹) for all relevant pairs of molecules in the crystal packing of **1** to **4**

CPD	E_{ele}	E_{pol}	E_{dis}	E_{rep}	E_{tot}	Symmetry ^a	Related H bonds (Table 4)
E64c (1)	-236.9	-52.7	-42.5	281.2	-160	Intra asu	O ₃ D-H ₁ AD...O ₅ C/ N ₁ D-H ₁ BD...O ₂ C/ C ₁ D-H ₁ DD...O ₂ C/ O ₅ D...H ₁ AC-O ₃ C/ O ₂ D...H ₁ BC-N ₁ C/ O ₂ D...H ₁ DC-C ₁ C
	-50.0	-16.0	-55.7	70.7	-70	$x, y, 1 + z$	N ₂ D-H ₁ CD...O ₄ B ^a
	-44.6	-14.7	-35.2	45.1	-61	$-1 + x, y, 1 + z$	O ₄ D...H ₁ CB ^a -N ₂ B ^a
	-6.1	-2.9	-23.5	12.9	-21	$1 + x, y, z$ (D)	None
						$-1 + x, y, z$ (D)	None
	-1.6	-3.4	-25.0	8.0	-21	$1 + x, y, z$ (C)	None
	-8.1	-1.7	-29.9	27.5	-19	$x, 1 + y, 1 + z$ (A)	None
	-3.6	-2.4	-25.0	13.6	-19	$-1 + x, 1 + y, 1 + z$ (B)	None
	-3.4	-1.9	-22.6	9.9	-18	$x, 1 + y, -1 + z$ (C)	None
	-2.5	-0.9	-22.4	14.0	-14	$x, 1 + y, 1 + z$ (B)	None
	E64d (2)	-76.9	-22.7	-61.3	90.2	-97	$1 + x, y, z$
						$-1 + x, y, z$	N ₂ -H ₂ N...O ₅ ^a
-1.9		-2.3	-41.4	14.8	-30	$2 - x, 1/2 + y, 3/2 - z$	None
						$2 - x, -1/2 + y, 3/2 - z$	None
-13.8		-4.4	-15.8	10.4	-25	$1/2 + x, 1/2 - y, 1 - z$	C ₁₆ -H ₁₆ A...O ₁ ^a
						$-1/2 + x, 1/2 - y, 1 - z$	None
					$1 - x, 1/2 + y, 3/2 - z$	None	
					$1 - x, -1/2 + y, 3/2 - z$	None	
VH04 (3)	-50.9	-11.1	-87.9	93.9	-81	$1 + x, y, z$	C ₅ -H ₅ ...O ₅ ^a
						$-1 + x, y, z$	N ₁ -H ₁ N...O ₄ ^a / C ₁ -H ₁ ...O ₄ ^a
	-17.0	-4.7	-19.2	15.6	-28	$1/2 + x, 3/2 - y, 2 - z$	C ₂₁ -H ₂₁ B...O ₂ ^a
						$-1/2 + x, 3/2 - y, 2 - z$	C ₂₁ -H ₂₁ B...O ₁ ^a
	-8.2	-2.9	-27.9	15.7	-25	$-x, 1/2 + y, 5/2 - z$	None
						$-x, -1/2 + y, 5/2 - z$	None
	-5.5	-1.5	-37.5	24.1	-24	$1/2 + x, 5/2 - y, 2 - z$	None
					$-1/2 + x, 5/2 - y, 2 - z$	None	
					$1 - x, 1/2 + y, 5/2 - z$	None	
					$1 - x, -1/2 + y, 5/2 - z$	None	
ASMC (4)	-65.3	-56.0	-5.7	7.7	-112	$-1/2 + x, 3/2 - y, -z$	O ₄ ...K ₁ ^a
	-124.8	-51.2	-8.1	123.5	-105	$1 - x, y, 1/2 - z$	O ₃ -H ₂ O...O ₅ ^a
	-46.7	-63.7	-11.4	10.8	-101	Intra asu	O ₁ ...K ₁ / O ₃ ...K ₁
	-46.1	-54.1	-6.6	11.5	-89	$-1/2 + x, 1/2 + y, z$	O ₂ ...K ₁ ^a
	-55.2	-36.3	-15.4	19.2	-88	$-1 + x, y, z$	N ₁ -H ₁ NA...O ₆ ^a
	-13.6	-32.5	-5.3	2.2	-42	$1/2 - x, 1/2 + y, 1/2 - z$	O ₂ ...K ₁ ^a
	-30.3	-6.5	-10.5	24.8	-31	$-1/2 + x, 3/2 - y, -z$	N ₁ -H ₁ NB...O ₁ ^a / N ₁ -H ₁ NB...O ₄ ^a
						$1/2 + x, 3/2 - y, -z$	None
	-1.4	-13.2	-14.7	8.8	-19	$-1/2 + x, -1/2 + y, z$ (TFA)	None
	-11.0	-2.0	-5.3	3.4	-16	$-1/2 + x, -1/2 + y, z$	N ₁ -H ₁ NA...O ₂ ^a
	29.9	-7.0	-3.7	0.5	24	$-1/2 + x, 3/2 - y, -z$ (TFA)	None
	32.5	-8.4	-2.1	1.8	28	$-1/2 + x, 1/2 + y, z$ (TFA)	None
	47.7	-16.3	-1.7	0.0	37	$-1 + x, y, z$ (K)	None

E_{ele} = electrostatic (Coulomb) interaction energy, E_{pol} = polarization, E_{dis} = dispersion, E_{rep} = repulsion, E_{tot} = total energy, calculated according to Turner et al.^[22] See Section 2 for more details. Note that the energy components are unscaled and hence not directly comparable, but the total energy is the sum of scaled components. Moreover, the model energies that refer to interactions involving charged species have not been calibrated or tested against theoretical dimer calculations in the way that those interactions involving only neutral species have been benchmarked by Turner et al.^[22] Hence, they have to be interpreted with care. For **1** and **3**, only the major disorder components were used in the calculations. For **1**, the calculations were only carried out with reference to molecule D. All results with total energies below an absolute value of 10 kJ mol⁻¹ were omitted. If there is more than one translation on top of a symmetry operation that leads to the same contact pair, all translations are given in order to relate to the hydrogen bonding pattern in Table 4. Each dimer represents all hydrogen bonds including the inverse of the contacts given for the other translation of the same symmetry operation if there is one.

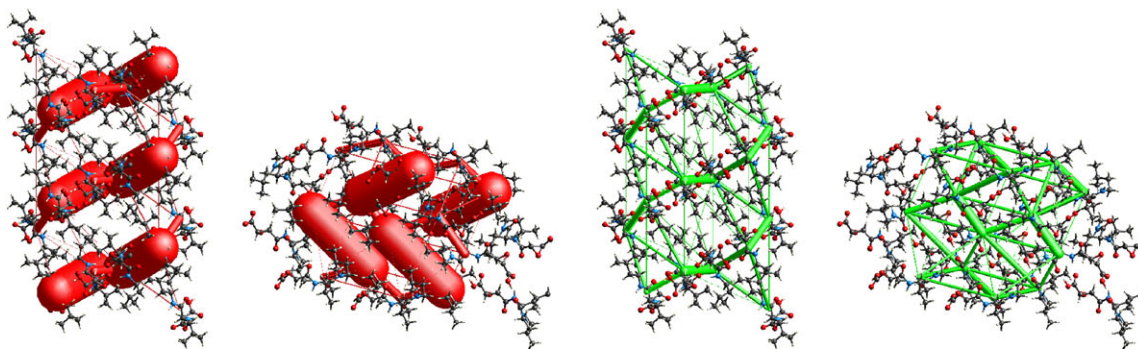
Abbreviations: asu, asymmetric unit; TFA, trifluoroacetate.

^aSymmetry operations refer to the atoms labelled with a.

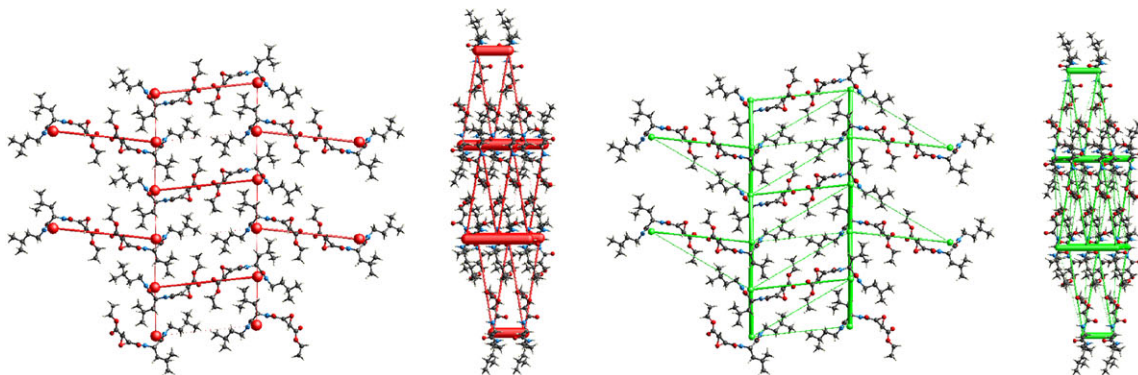
contacts have already been identified. However, this does not necessarily mean that those contacts have the largest negative total energies, since there are a few pairwise interactions that are dominated by strongly attractive dispersion interactions; see E64d and ASMC. These molecular pairs are certainly as stabilizing to the crystal packing as those that are dominated by electrostatics but would never be listed in a table such as Table 4 that focuses on atom-atom interactions.

Figure 1 shows that the biologically most important hydrogen bonds are any of the conventional ones except those involving the epoxide as well as the amide (in **1** and **2**) or ester (in **3**) groups that do not belong to the *trans*-

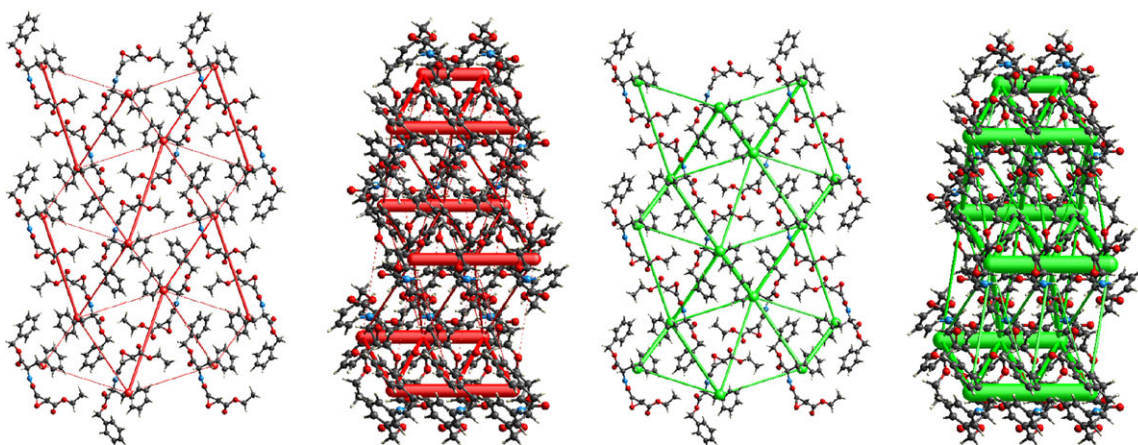
epoxysuccinyl amide moiety. Nevertheless, these groups are part of the interaction networks in the crystals. It is therefore hard to interpret these networks according to the biological activity, and inadequate to only focus on atom-atom interactions as the discussion about the ESP and Politzer parameters above and the discussion in the previous paragraph have shown. However, Table 5 does highlight the importance of the interactions of the carboxyl group in terms of the hydrogen bonds O₃-H₁A/H₂O...O₅. They only occur in E64c and ASMC since E64d and VH04 are esters, and they are by far the strongest interactions in terms of electrostatics. In E64c, two of these hydrogen bonds form within a dimer of



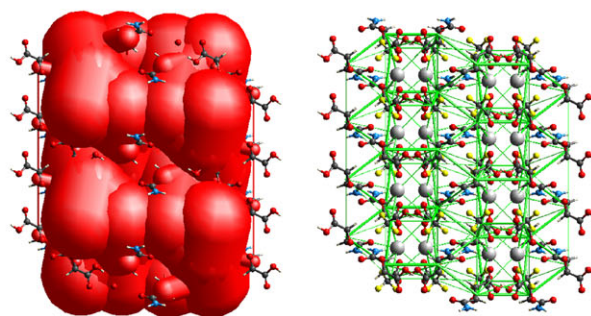
(A) E64c (**1**): Coulomb and dispersion energies down axes *a* and *b* each



(B) E64d (**2**): Coulomb and dispersion energies down axes *a* and *b* each



(C) VH04 (**3**): Coulomb and dispersion energies down axes *a* and *b* each



(D) ASMC (**4**) with potassium trifluoroacetate: Coulomb and dispersion energies down axis *a*

FIGURE 6 Energy framework plots as visualization of Table 5 for compounds **1** to **4** with a CrystalExplorer tube size scale factor of 10. For **1** and **3**, only the major disorder components were used in the calculations. Red = electrostatic (Coulomb) energies, green = dispersion energies. The total energies and missing orientations are shown in the Supporting Information. Only negative, ie, attractive or binding, energies are represented, whereas positive, ie, repulsive, energies are omitted

neutral molecules together with two other weaker hydrogen bonds. In ASMC, O_3-H_2O interacts with an anion, O_5 in trifluoroacetate, but the electrostatic term is the highest in both cases and the total energy is likewise large and negative, showing that $O_3-H_2O...O_5$ is certainly a structure-determining motif. This agrees with the analysis of fingerprint plots discussed above (Figure 5A and D) where E64c and ASMC are most similar in terms of their shortest interactions. It can be concluded that the carboxyl group is the anchor that binds the low-molecular weight ligand to the enzyme pocket and rationalizes why the ester compounds do not show significant biological activity. On the basis of this analysis, in a subsequent study, we will use ASMC as a model compound in molecular dynamics and quantum mechanics/molecular mechanics calculations with the enzyme to investigate the role of the carboxyl group in more detail.

A visualization of the energies listed in Table 5 is possible through energy framework representations that were recently introduced.^[23] Figure 6 shows that electrostatics (red) dominate the crystal packing in E64c (**1**) and ASMC (**4**)—the latter involving ionic species including anion-cation interactions that are not listed in Table 5, so direct comparability is not given—but dispersion slightly exceeds electrostatic contributions in the crystal packing of VH04 (**3**). The huge difference between E64c (Figure 6A) on the one hand and E64d and VH04 on the other hand (Figure 6B and C) again highlights the special importance of electrostatic interactions involving the carboxyl group. Another difference between E64c (**1**) and the ester compounds is that in the latter electrostatics and dispersion show the same pattern, which means they reinforce and strengthen the same intermolecular interactions. In other words, in the direction where electrostatics are strongest, dispersion is strongest as well. This is different in E64c, where electrostatics and dispersion complement each other; where electrostatics are strongest, dispersion is weakest, and vice versa.

4 | CONCLUSIONS

Invariance applications and isolated-molecule calculations do not account for the environment; they only detect substituent effects in the ED. In this study, precisely this fact made them valuable in allowing a clear separation between crystal packing effects and substituent effects on the biologically and pharmaceutically important *trans*-epoxysuccinyl amide moiety. Using these techniques, we found that for the *trans*-epoxysuccinyl amide group, it is mainly not the substituent effects but the environment that determines differences between geometrical arrangements and changes in the ED distribution in the region of interest among the investigated compounds **1** to **4**. Only by using Politzer's internal polarization parameter Π could a connection between the strong biological activity of E64c (**1**) and the weak or in-existent activities of **2** to **4** be drawn. However, with inherent

electronic or electrostatic properties, it cannot be rationalized that the nucleophilic ring-opening reaction takes place at carbon atom C_2 under cleavage of C_2-O_1 . Having confirmation that the environment is decisive for the reactivity of the *trans*-epoxysuccinyl amide group, and knowing from previous work that the crystalline environment is a very good approximation for the enzyme environment in the case of E64c (**1**),^[14] the necessity for future experimental ED investigations of *trans*-epoxysuccinyl amide model compounds based on single-crystal X-ray diffraction becomes even more obvious.

In order to determine if the model compounds VH04 (**3**) and ASMC (**4**) that were synthesized within this study can be used for future experiments, their intermolecular interaction patterns were scrutinized in detail and compared with E64c (**1**) and E64d (**2**). The interactions of the carboxyl group prove to be the decisive features that govern the biological activity of E64c relative to the ethyl esters VH04 and E64d. For this reason, ASMC, which incorporates the carboxyl group, shows promising features in terms of intermolecular interactions and energies despite its small size. The investigation of substituent effects as discussed in the previous paragraph has also shown that it is justified to investigate a small model compound since the substituents themselves do not influence the electronic situation in the *trans*-epoxysuccinyl amide region significantly. This prompts us to further investigate experimental conditions for growing ASMC crystals whose properties are more suited than in the case of the present cocrystal with potassium trifluoroacetate. We will start further attempts to crystallize ASMC in its deprotonated form with various cations (cationic amino acids such as histidinium, metal ions in aqueous solution to provoke cocrystallization with water, etc) to obtain good crystal quality for high-resolution experiments and simultaneously an interaction pattern as similar as possible to that of deprotonated E64c in the enzyme.

ACKNOWLEDGEMENTS

S. Grabowsky and M. A. Spackman thank the Australian Research Council (ARC) for funding this project within the Discovery Project DP130103488. S. Grabowsky further acknowledges the financial support of the ARC within the Discovery Early Career Researcher Award (DECRA) DE140101330 and of the German Research Foundation (Deutsche Forschungsgemeinschaft DFG) within the Emmy Noether project GR 4451/1-1. B. Dittrich acknowledges funding within the DFG Project DI 921/6-1, and P. R. Spackman acknowledges the financial support of the Danish National Research Foundation (Center for Materials Crystallography, DNRF-93). ChemMatCARS Sector 15 is principally supported by the Divisions of Chemistry (CHE) and Materials Research (DMR), National Science Foundation, under grant number NSF/CHE-1346572. Use of the Advanced Photon Source, an Office of Science User Facility operated for the US Department of Energy (DOE) Office of

Science by Argonne National Laboratory, was supported by the US DOE under contract no. DE-AC02-06CH11357. The authors acknowledge the X-ray diffraction and NMR facilities as well as the scientific and technical assistance of the Centre for Microscopy, Characterisation and Analysis, The University of Western Australia, a facility funded by the University, State and Commonwealth Governments, especially the help of and discussion with Dr Lindsay Byrne. We moreover thank Prof Murray Baker for his suggestions regarding the stereochemistry of the synthesized products.

REFERENCES

- [1] a) B. J. Gour-Salin, P. Lachance, C. Plouffe, A. C. Storer, R. Menard, *J. Med. Chem.* **1993**, *36*, 720; b) H.-H. Otto, T. Schirmeister, *Chem. Rev.* **1997**, *97*, 133; c) J. C. Powers, J. L. Asgian, Ö. D. Ekici, K. E. James, *Chem. Rev.* **2002**, *102*, 4639;
- [2] a) B. M. Dunn, *Chem. Rev.* **2002**, *102*, 4431; b) B. Degel, P. Staib, S. Rohrer, J. Scheiber, E. Martina, C. Büchold, K. Baumann, J. Morschhäuser, T. Schirmeister, *Chem. Med. Chem.* **2008**, *3*, 302; c) C. Büchold, Y. Hemberger, C. Heindl, A. Welker, B. Degel, T. Pfeuffer, P. Staib, S. Schneider, P. J. Rosenthal, J. Gut, C. Sotriffer, J. Morschhäuser, G. Bringmann, T. Schirmeister, *Chem. Med. Chem.* **2011**, *6*, 141;
- [3] K. Hanada, M. Tamai, M. Yamagishi, S. Ohmura, J. Sawada, I. Tanaka, *Agric. Biol. Chem.* **1978**, *42*, 523;
- [4] a) N. Schaschke, D. Deluca, I. Assfalg-Machleidt, C. Höhneke, C. P. Sommerhoff, W. Machleidt, *Chem. Biol.* **2002**, *383*, 849; b) C. Czaplewski, Z. Grzonka, M. Jaskólski, F. Kasprzykowski, M. Kozak, E. Politowska, J. Ciarkowski, *Biochim. Biophys. Acta* **1999**, *1431*, 290; c) M. Murata, S. Miyashita, C. Yokoo, M. Tamai, K. Hanada, K. Hatayama, T. Towatari, T. Nikawa, N. Katunuma, *FEBS Lett.* **1991**, *280*, 307; d) T. Towatari, T. Nikawa, M. Murata, C. Yokoo, M. Tamai, K. Hanada, N. Katunuma, *FEBS Lett.* **1991**, *280*, 311; e) A. J. Barrett, A. A. Kumbhavi, M. A. Brown, H. Kirschke, C. G. Knight, M. Tamai, K. Hanada, *Biochem. J.* **1982**, *201*, 189; f) N. Schaschke, I. Assfalg-Machleidt, W. Machleidt, T. Laßleben, C. P. Sommerhoff, L. Moroder, *Bioorg. Med. Chem. Lett.* **2000**, *10*, 677; g) H. Sugita, S. Ishiura, K. Suzuki, K. Imahori, *J. Biochem.* **1980**, *87*, 339; h) S. Hashida, T. Towatari, E. Kominami, N. Katunuma, *J. Biochem.* **1980**, *88*, 1805; i) K. Suzuki, S. Tsuji, S. Ishiura, *FEBS Lett.* **1981**, *136*, 119; j) C. Parkes, A. A. Kumbhavi, A. J. Barrett, *Biochem. J.* **1985**, *230*, 509; k) B. J. Goursalin, P. Lachance, P. R. Bonneau, A. C. Storer, H. Kirschke, D. Brömme, *Bioorg. Chem.* **1994**, *22*, 227; l) I. Santamaria, G. Velasco, A. M. Pendas, A. Paz, C. Lopez-Otin, *J. Biol. Chem.* **1999**, *274*, 13800;
- [5] N. D. Rawlings, M. Waller, A. J. Barrett, A. Bateman, *Nucleic Acids Res.* **2014**, *42*, D503;
- [6] a) S. Hashida, T. Towatari, E. Kominami, N. Katunuma, *J. Biochem.* **1980**, *88*, 1805; b) T. Noda, K. Kazuhide, N. Katunuma, Y. Tarumoto, M. Ohezeki, *J. Biochem.* **1981**, *90*, 893; c) K. Suzuki, *J. Biochem.* **1983**, *93*, 1305; d) D. H. Hu, S. Kimura, S. Kawashima, K. Maruyama, *Zoolog. Sci.* **1989**, *6*, 797; e) Z. Huang, E. B. McGowan, T. C. Detwiler, *J. Med. Chem.* **1992**, *35*, 2048;
- [7] a) K. Matsumoto, D. Yamamoto, H. Ohishi, K. Tomoo, T. Ishida, M. Inoue, T. Sadatome, K. Kitamura, H. Mizuno, *FEBS Lett.* **1989**, *245*, 177; b) M. J. Kim, D. Yamamoto, K. Matsumoto, M. Inoue, T. Ishida, H. Mizuno, S. Sumiya, K. Kitamura, *Biochem. J.* **1992**, *287*, 797; c) J. P. Meara, D. H. Rich, *J. Med. Chem.* **1996**, *39*, 3357; d) A. Yamamoto, K. Tomoo, K. Matsugi, T. Hara, Y. In, M. Murata, K. Kitamura, T. Ishida, *Biochim. Biophys. Acta* **2002**, *1597*, 244; e) M. Mladenovic, K. Junold, R. F. Fink, W. Thiel, T. Schirmeister, B. Engels, *J. Phys. Chem. B.* **2008**, *112*, 5458;
- [8] a) N. Schaschke, I. Assfalg-Machleidt, W. Machleidt, D. Turk, L. Moroder, *Bioorg. Med. Chem.* **1997**, *5*, 1789; b) M. Mladenovic, K. Ansgor, R. F. Fink, W. Thiel, T. Schirmeister, B. Engels, *J. Phys. Chem. B.* **2008**, *112*, 11798;
- [9] a) C. Pascard, *Acta Cryst. D* **1995**, *51*, 407; b) G. Klebe, chapter 13, *Structure Correlation and Ligand/Receptor Interactions*, in: *Structure Correlation*, (Eds: H.-B. Bürgi, J. D. Dunitz) Vol. 1, Wiley-VCH, Weinheim **2008**.
- [10] a) D. Parrish, E. A. Zhurova, K. Kirschbaum, A. A. Pinkerton, *J. Phys. Chem. B* **2006**, *110*, 26442; b) E. A. Zhurova, C. F. Matta, N. Wu, V. V. Zhurov, A. A. Pinkerton, *J. Am. Chem. Soc.* **2006**, *128*, 8849; c) E. J. Yearly, E. A. Zhurova, V. V. Zhurov, A. A. Pinkerton, *J. Am. Chem. Soc.* **2007**, *129*, 15013; d) R. Destro, R. Soave, M. Barzaghi, L. Lo Presti, *Chem. – Eur. J.* **2007**, *13*, 6942; e) J. Overgaard, I. Turel, D. E. Hibbs, *Dalton Trans.* **2007**, 2171; f) D. E. Hibbs, J. Overgaard, S. T. Howard, T. H. Nguyen, *Org. Biomol. Chem.* **2005**, *3*, 441; g) N. Zhu, C. L. Klein Stevens, E. D. Stevens, *J. Chem. Cryst.* **2005**, *35*, 13; h) L. Lo Presti, R. Soave, R. Destro, *J. Phys. Chem. B* **2006**, *110*, 6405;
- [11] a) P. Luger, *Org. Biomol. Chem.* **2007**, *5*, 2529; b) P. Luger, M. Weber, B. Dittrich, *Future Med. Chem.* **2012**, *4*, 1399;
- [12] a) M. Mladenovic, M. Arnone, R. F. Fink, B. Engels, *J. Phys. Chem. B.* **2009**, *113*, 5072; b) B. Engels, T. C. Schmidt, C. Gatti, T. Schirmeister, R. F. Fink, *Struct. Bonding* **2012**, *147*, 47; c) S. Grabowsky, D. Jayatilaka, R. F. Fink, T. Schirmeister, B. Engels, *Z. Anorg. Allg. Chem.* **2013**, *639*, 1905;
- [13] a) S. Grabowsky, T. Pfeuffer, W. Morgenroth, C. Paulmann, T. Schirmeister, P. Luger, *Org. Biomol. Chem.* **2008**, *6*, 2295; b) S. Grabowsky, T. Schirmeister, C. Paulmann, T. Pfeuffer, P. Luger, *J. Org. Chem.* **2011**, *76*, 1305;
- [14] M. W. Shi, A. N. Sobolev, T. Schirmeister, B. Engels, T. C. Schmidt, P. Luger, S. Mebs, B. Dittrich, Y.-S. Chen, J. M. Bąk, D. Jayatilaka, C. S. Bond, M. J. Turner, S. G. Stewart, M. A. Spackman, S. Grabowsky, *New J. Chem.* **2015**, *39*, 1628;
- [15] a) B. Dittrich, C. B. Hübschle, K. Pröpper, F. Dietrich, T. Stolper, J. J. Holstein, *Acta Cryst. B* **2013**, *69*, 91; b) B. Dittrich, T. Koritsánszky, P. Luger, *Angew. Chem. Int. Ed.* **2004**, *43*, 2718;
- [16] C. B. Hübschle, P. Luger, B. Dittrich, *J. Appl. Crystallogr.* **2007**, *40*, 623;
- [17] a) P. Luger, M. Weber, C. B. Hübschle, R. Tacke, *Org. Biomol. Chem.* **2013**, *11*, 2348; b) M. Weber, S. Grabowsky, A. Hazra, S. Naskar, S. Banerjee, N. B. Mondal, P. Luger, *Chem. – Asian J.* **2011**, *6*, 1390; c) B. Dittrich, M. Weber, R. Kalinowski, S. Grabowsky, C. B. Hübschle, P. Luger, *Acta Cryst. B* **2009**, *65*, 749; d) B. Dittrich, C. B. Hübschle, J. J. Holstein, F. P. A. Fabbiani, *J. Appl. Crystallogr.* **2009**, *42*, 1110;
- [18] B. Dittrich, C. Schürmann, C. B. Hübschle, *Z. Kristallogr.* **2016**, *231*, 725.
- [19] T. Ishida, M. Sakaguchi, D. Yamamoto, M. Inoue, K. Kitamura, K. Hanada, T. Sadatome, *J. Chem. Soc. Perkin Trans.* **1988**, *6*, 851;
- [20] a) R. F. W. Bader, *Atoms in Molecules. A Quantum Theory*, Oxford University Press, Oxford, U. K. **1990**; b) R. F. W. Bader, *Chem. Rev.* **1991**, *91*, 893;
- [21] a) M. A. Spackman, D. Jayatilaka, *Cryst. Eng. Comm.* **2009**, *11*, 19; b) J. J. McKinnon, D. Jayatilaka, M. A. Spackman, *Chem. Commun.* **2007**, 3814; c) J. J. McKinnon, M. A. Spackman, A. S. Mitchell, *Acta Cryst. B* **2004**, *60*, 627; d) J. J. McKinnon, A. S. Mitchell, M. A. Spackman, *Chem. – Eur. J.* **1998**, *4*, 2136;
- [22] M. J. Turner, S. Grabowsky, D. Jayatilaka, M. A. Spackman, *J. Phys. Chem. Lett.* **2014**, *5*, 4249;
- [23] a) M. J. Turner, S. P. Thomas, M. W. Shi, D. Jayatilaka, M. A. Spackman, *Chem. Commun.* **2015**, *51*, 3735; b) M. W. Shi, S. P. Thomas, G. Koutsantonis, M. A. Spackman, *Cryst. Growth Des.* **2015**, *15*, 5892;
- [24] M. J. Turner, J. J. McKinnon, S. K. Wolff, D. J. Grimwood, P. R. Spackman, D. Jayatilaka, M. A. Spackman, *CrystalExplorer*, The University of Western Australia **2016**, version 3.3;
- [25] S. Saito, K. Komada, T. Moriwake, *Org. Synth.* **1996**, *73*, 184;
- [26] An accurate yield was not achieved because of the incomplete removal of CF₃COOH.
- [27] T. Schirmeister, M. Peric, *Bioorg. Med. Chem.* **2000**, *8*, 1281;
- [28] a) G. M. Sheldrick, *Acta Cryst. A* **2008**, *64*, 112; b) G. M. Sheldrick, *Acta Cryst. C* **2015**, *71*, 3;
- [29] C. B. Hübschle, G. M. Sheldrick, B. Dittrich, *J. Appl. Crystallogr.* **2011**, *44*, 1281;

- [30] A. Volkov, P. Macchi, L. J. Farrugia, C. Gatti, P. R. Mallinson, T. Richter, T. S. Koritsánszky, *XD2006, A Computer Program for Multipole Refinement, Topological Analysis, and Evaluation of Intermolecular Energies from Experimental and Theoretical Structure Factors*, University at Buffalo, NY, USA **2006**;
- [31] C. B. Hübschle, P. Luger, *J. Appl. Crystallogr.* **2006**, *39*, 901;
- [32] M. J. Frisch, G. W. Trucks, H. B. Schlegel, G. E. Scuseria, M. A. Robb, J. R. Cheeseman, G. Scalmani, V. Barone, B. Mennucci, G. A. Petersson, H. Nakatsuji, M. Caricato, X. Li, H. P. Hratchian, A. F. Izmaylov, J. Bloino, G. Zheng, J. L. Sonnenberg, M. Hada, M. Ehara, K. Toyota, R. Fukuda, J. Hasegawa, M. Ishida, T. Nakajima, Y. Honda, O. Kitao, H. Nakai, T. Vreven, J. A. Montgomery, J. E. Peralta, F. Ogliaro, M. Bearpark, J. J. Heyd, E. Brothers, K. N. Kudin, V. N. Staroverov, T. Keith, R. Kobayashi, J. Normand, K. Raghavachari, A. Rendell, J. C. Burant, S. S. Iyengar, J. Tomasi, M. Cossi, N. Rega, J. M. Millam, M. Klene, J. E. Knox, J. B. Cross, V. Bakken, C. Adamo, J. Jaramillo, R. Gomperts, R. E. Stratmann, O. Yazyev, A. J. Austin, R. Cammi, C. Pomelli, J. W. Ochterski, R. L. Martin, K. Morokuma, V. G. Zakrzewski, G. A. Voth, P. Salvador, J. J. Dannenberg, S. Dapprich, A. D. Daniels, O. Farkas, J. B. Foresman, J. V. Ortiz, J. Cioslowski, D. J. Fox, *Gaussian 09*, Gaussian, Inc., Wallingford CT, USA **2013**, Revision D.01;
- [33] F. Biegler-König, J. Schönbohm, D. Bayles, *J. Comput. Chem.* **2001**, *22*, 545;
- [34] S. Grabowsky, M. Weber, J. Buschmann, P. Luger, *Acta Cryst. B* **2008**, *64*, 397;
- [35] S. Grabowsky, D. Jayatilaka, S. Mebs, P. Luger, *Chem. – Eur. J.* **2010**, *16*, 12818;
- [36] a) J. Henn, D. Ilge, D. Leusser, D. Stalke, B. Engels, *J. Phys. Chem. A* **2004**, *108*, 9442; b) S. Grabowsky, D. Kalinowski, M. Weber, D. Förster, C. Paulmann, P. Luger, *Acta Cryst. B* **2009**, *65*, 488; c) A. Volkov, P. Coppens, *Acta Cryst. A* **2001**, *57*, 395; d) A. Volkov, Y. Abramov, P. Coppens, C. Gatti, *Acta Cryst. A* **2000**, *56*, 332;
- [37] a) A. Fischer, D. Tiana, W. Scherer, K. Batke, G. Eickerling, H. Svendsen, N. Bindzus, B. B. Iversen, *J. Phys. Chem. A* **2011**, *115*, 13061; b) K. Batke, G. Eickerling, *J. Phys. Chem. A* **2013**, *117*, 11566; c) T. Koritsánszky, A. Volkov, M. Chodkiewicz, *Struct. Bonding* **2012**, *147*, 1;
- [38] a) S. Grabowsky, P. Luger, J. Buschmann, T. Schneider, T. Schirmeister, A. N. Sobolev, D. Jayatilaka, *Angew. Chem. Int. Ed.* **2012**, *51*, 6776; b) L. Chęcińska, W. Morgenroth, C. Paulmann, D. Jayatilaka, B. Dittrich, *Cryst. Eng. Comm.* **2013**, *15*, 2084;
- [39] a) B. Zarychta, V. Pichon-Pesme, B. Guillot, C. Lecomte, C. Jelsch, *Acta Cryst. A* **2007**, *63*, 108; b) A. Volkov, M. Messerschmidt, P. Coppens, *Acta Cryst. D* **2007**, *63*, 160;
- [40] a) M. A. Spackman, P. G. Byrom, *Chem. Phys. Lett.* **1997**, *267*, 215; b) M. A. Spackman, J. J. McKinnon, D. Jayatilaka, *Cryst. Eng. Comm.* **2008**, *10*, 377;
- [41] a) J. J. Holstein, C. B. Hübschle, B. Dittrich, *Cryst. Eng. Comm.* **2012**, *14*, 2520; b) K. Pröpper, J. J. Holstein, C. B. Hübschle, C. S. Bond, B. Dittrich, *Acta Cryst. D* **2013**, *69*, 1530;
- [42] P. Politzer, J. S. Murray, Z. Peralta-Inga, *Int. J. Quant. Chem.* **2001**, *85*, 676;
- [43] T. H. Schneider, M. Rieger, K. Ansorg, A. N. Sobolev, T. Schirmeister, B. Engels, S. Grabowsky, *New J. Chem.* **2015**, *39*, 5841;

SUPPORTING INFORMATION

Additional Supporting Information may be found online in the supporting information tab for this article.

How to cite this article: Shi MW, Stewart SG, Sobolev AN, Dittrich B, Schirmeister T, Luger P, Hesse M, Chen Y-S, Spackman PR, Spackman MA, Grabowsky S. Approaching an experimental electron density model of the biologically active *trans*-epoxysuccinyl amide group—Substituent effects vs. crystal packing. *J Phys Org Chem.* 2017;e3683. <https://doi.org/10.1002/poc.3683>